IEEE Access
Multidisciplinary | Rapid Review | Open Access Journal

Received April 9, 2019, accepted April 21, 2019, date of publication April 25, 2019, date of current version May 28, 2019.

Digital Object Identifier 10.1109/ACCESS.2019.2913164

Open-Switch Fault Diagnosis Method in Voltage-Source Inverters Based on Phase Currents

ZHANG JIAN-JIAN[1,2], CHEN YONG[1,2], (Senior Member, IEEE), CHEN ZHANG-YONG[1,2], AND ZHOU ANJIAN[3]

[1]School of Automation Engineering, University of Electronic Science and Technology of China (UESTC), Chengdu 611731, China
[2]Institute of Electric Vehicle Driving System and Safety Technology, University of Electronic Science and Technology of China (UESTC), Chengdu 611731, China
[3]Chongqing Changan Automobile Co., Ltd., Chongqing 400023, China

Corresponding author: Chen Yong (ychencd@uestc.edu.cn)

This work was supported in part by the National Key Research and Development Plan Programs of China under Grant 2018YFB0106101, in part by the National Natural Science Foundation of China under Grant 51607027, in part by the Scientific and Technical Supporting Programs of Sichuan Province of China under Grant 2016GZ0395, Grant 2017GZ0394, and Grant 2017GZ0395, and in part by the Fundamental Research Funds for the Central Universities under Project ZYGX2016J140 and Project ZYGX2016J146.

ABSTRACT Presently, condition monitoring and fault diagnostics in the three-phase voltage-source inverter (VSI) system are already considered essential to improve maintenance efficiency and increase reliability levels. This paper presents a new open-switch fault real-time diagnosis method in the VSI based on the phase currents. First, on the basis of real-time measured two phase currents, the sum of the absolute value of the normalized phase currents is calculated, whose average value is less relevant to the transient condition such as load variations and current frequency variations. Second, the current zero-cross detection method is employed to avoid the influence of current distortion caused by the transient condition. Then, the fault detection signal is built to precisely localize the faulty switches, and the real-time fast diagnosis for three-phase VSI with the open-switch fault is realized. Finally, the experiment results verify the reliability and effectiveness of the proposed method.

INDEX TERMS Voltage-source inverter, open-switch, fault diagnosis, load variations, current frequency variations.

I. INTRODUCTION

Because of the increasingly severe energy crisis in today's society, power electronics technology has been extensively applied in the fields of Smart Grid, new energy power generation and rail traffic, among which the voltage-source inverter plays a prominent role. However, the semiconductor power device fault will bring about an inevitably destructive damage to the system, especially for the unnoticeable open circuit fault [1]–[3]. Therefore, this paper studies the current characteristics of three phase inverter system and presents an accurate and fast fault diagnosis method, which possesses both theoretical and practical significances [4].

The average value of the normalized converter phase currents and the absolute normalized currents were employed as principal quantities to formulate the diagnostic variables in [5]. Through the diagnostic variables and the adaptive threshold, the method for open-switch faults in the back-to-back converter of a doubly fed wind turbine can realize the detection and identification of single and multiple open-switch faults. An online diagnosis method was presented for three-phase PWM voltage source rectifier system in [6]. The current distortion was used in the proposed method to diagnose faults. The proposed method can diagnose the faulty switch at low currents as well as under abrupt load transient conditions without false alarms. However, it only can realize the diagnosis of single open-switch fault. Through analyzing the impact of open-switch switch failures of the series-connected identical submodules (SMs) on the operation of the modular multilevel converter (MMC), a clustering algorithm-based method and a calculated capacitance-based method were proposed in [7]. Based on the normalized dc-components method, the average absolute values are employed instead of using the fundamental components as

The associate editor coordinating the review of this manuscript and approving it for publication was Youqing Wang.

the normalizing quantities in [8]. By combining the normalized average currents with additional diagnostic variables, the certainty of the diagnoses under transients and light loads had been improved. The fault diagnosis method based on the slope of the current-vector trajectory were proposed in [9], which was independent of the mathematical model and load transient characteristic while required longer diagnosis time (around 1.5 to 2 times of current fundamental period).

The current Park's vector phase for inverter open-switch fault diagnosis was presented in [11]–[13]. In [11], the authors compared and analyzed several different current Park's vector phase approaches. The proposed methods were suitable for integration into the drive controller and triggering remedial actions. In [12], the Park's vector normalized currents and errors of their average absolute values were utilized to improve the processing speed. The proposed method can allow for the diagnosis of single and multiple open-switch failures. In [13], a method suitable for closed-loop system was exhibited which avoided extra current sensors or electric devices and was independent of load and rotating speed. Besides, it can handle the extremely transient condition within short diagnosis time. Nevertheless, this method is not fit for open-loop control such as V/F control system.

In order to reduce the amount of additional hardware, the observer-based diagnostic methods were introduced for open-switch faults in [10], [14]–[18]. The residual values between the actual signal and the observation signal were used to detect the faulty switches. A nonlinear current observer and the residual evaluation in the dq-frame were employed to detect faults in [10] and [14], and these residuals are constructed to identify the faulty switches in at least one fundamental period. Based on the state space model, a Luenberger observer is used to observe the output current of three-phase inverter in [15], [16]. The current residuals were used to design the normalized current factor and adaptive threshold which can be constructed to detect open-switch faults. The hybrid system is adopted in three-phase VSI and according to the fault model of inverter the fault events collection and fault model are determined in [17]. An observer is used to estimate the phase voltages from a model based on Fourier coefficients of the BLDC motor waveform in [18].

A knowledge-based diagnosis method was adopted in [19]–[22], where [19] used the current pattern recognition method, [20] used the wavelet fuzzy logic method, [21] and [22] adopt the wavelet neural network method. These series of methods do not depend on the system model whereas the complex computations increase the diagnosis time.

In this paper, a novel real-time open-switch fault diagnosis method in three phase inverter is proposed, which holds advantages of simple operation, fast diagnosis and free from load transient. The phase current analysis of VSI will be introduced in Section II. In Section III, the detection and localization method will be presented. To test and validate the proposed method, the simulation and experimental results are given in Section IV and V, besides a false detection is checked under sudden load transient in this section by comparing with several previous methods. Finally, the conclusions will be summarized in the last section.

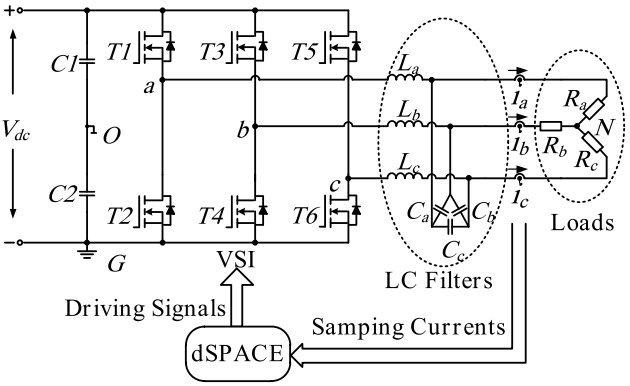

FIGURE 1. The three-phase voltage-source inverter system with dSPACE controller.

II. PHASE CURRENT ANALYSIS OF VSI

The three-phase voltage-source inverter system adopted in this paper is shown in Fig.1, which includes LC filters and dSPACE controller. The system sampling signal processing and control for VSI is implemented by dSPACE controller.

In the normal operation mode, the modulating signals of three phases fed by Pulse-Width-Modulation (PWM) differ 120 electrical degrees from each other. The drive signals for the upper and bottom switches of same phase are complementary. The output three phase currents are sinusoidal of same magnitude and phase difference with 120 electrical degrees, which is:

$$\begin{cases} i_a = I_m \sin(\omega t) \\ i_b = I_m \sin(\omega t - \dfrac{2\pi}{3}) \\ i_c = I_m \sin(\omega t + \dfrac{2\pi}{3}) \end{cases} \tag{1}$$

where I_m is the magnitude of current and ω is the current angular frequency.

Take an open-switch fault in the phase b bottom switch as an example. In the negative half cycle of the current, the current in this phase is strongly affected, so the current of phase b is zero during its negative half-cycle. Under these conditions, during one fundamental period, the current of phase b can be given by

$$i_b = \begin{cases} I_m \sin(\omega t - \dfrac{2\pi}{3}), & \dfrac{2\pi}{3\omega} < t \le \dfrac{5\pi}{3\omega} \\ 0, & \dfrac{5\pi}{3\omega} < t \le \dfrac{8\pi}{3\omega} \end{cases} \tag{2}$$

Through above analyses, on the basis of measured currents, the fault can be diagnosed using methods such as signal processing, coordinate transformation and pattern recognition etc [23]–[25].

III. FAULT DIAGNOSTIC METHOD

Generally, in a typical VSI, if an open-switch fault occurs in an upper switch, the current in that phase will only take negative values. Otherwise, if a fault occurs in a bottom switch, the

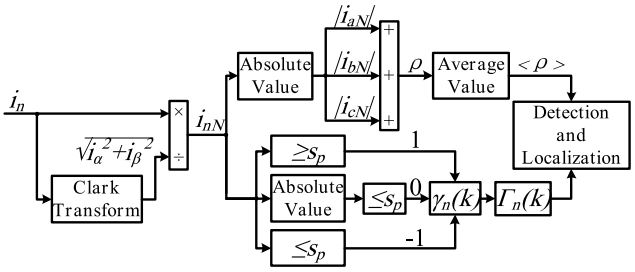

FIGURE 2. Block diagram of fault detection and localization method.

current in that phase will only take positive values. Therefore, the fault localization can be conducted based on the above-mentioned current characteristics. The block diagram of fault detection and localization method is exhibited in Fig.2.

A. FAULT DETECTION METHOD

The output currents of VSI are state parameters that cannot reflect the fault information on time. And the output current based diagnosis method is dependent of fundamental period. Hence, this paper proposes a novel detection method.

Since current amplitude is often related to the load and other factors, in order to make the algorithm overcome the impact of load change and other factors, simplify the diagnosis method, the current is normalized. Through Clark transform, the three-phase current is transformed from three-phase static coordinate system to two-phase static coordinate system:

$$\begin{cases} i_\alpha = \dfrac{2}{3}\left(i_a - \dfrac{1}{2}i_b - \dfrac{1}{2}i_c\right) \\ i_\beta = \dfrac{2}{3}\left(\dfrac{\sqrt{3}}{2}i_b - \dfrac{\sqrt{3}}{2}i_c\right) \end{cases} \tag{3}$$

The current can be handled with normalization method, which is:

$$i_{nN} = \frac{i_n}{\sqrt{i_\alpha^2 + i_\beta^2}} = \begin{cases} i_{a\mathrm{N}} = \sin(\omega t) \\ i_{b\mathrm{N}} = \sin(\omega t - \dfrac{2\pi}{3}) \\ i_{c\mathrm{N}} = \sin(\omega t + \dfrac{2\pi}{3}) \end{cases} \tag{4}$$

Here, we define

$$\rho = |i_{aN}| + |i_{\mathrm{bN}}| + |i_{cN}| \tag{5}$$

Substitute equation (4) into (5), therefore:

$$\rho = 2\sin(\omega t + \frac{k\pi}{3}), \quad \frac{k\pi}{\omega} < t \leq \frac{(k+1)\pi}{\omega} \tag{6}$$

where k = 0, 1, 2,... As can be observed from equation (4) that ρ is a periodic function whose period is 1/6 of the current fundamental period, and its average value is:

$$\begin{aligned} \langle\rho\rangle &= \frac{1}{T_1}\int_0^{T_1} \rho dt = \frac{1}{\frac{\pi}{3}}\int_{\frac{k\pi}{3}}^{\frac{(k+1)\pi}{3}} 2\sin(\omega t + \frac{k\pi}{3}) d(\omega t) \\ &= \frac{6}{\pi} \approx 1.91 \end{aligned} \tag{7}$$

However, when the three-phase VSI open-switch fault happens, the current will not be the same as shown in equation (6) and its value will descend rapidly. Therefore, the diagnostic variable can be reconfigured as:

$$F_d = \begin{cases} 1, & \langle\rho\rangle \leq s_d \\ 0, & \langle\rho\rangle > s_d \end{cases} \tag{8}$$

where s_d is the threshold value. When $F_d = 0$ it is under normal operation and when $F_d = 1$ there is an open-switch fault, which realizes a fast fault diagnosis of inverter. The threshold value is properly determined through comprehensively considering the variable change under normal and fault condition and making compromise between rapidity and reliability so as to avoid the false detection. Due to the applied normalization method, the threshold value will not be affected by different faults. Therefore, s_d can be fixed and it is selected as 1.8 in the following simulations and experiments. Take the bottom switch fault of phase *b* as an example, where the state of T4 is 'on'. The value of $\langle\rho\rangle$ will decreased rapidly and is lower than s_d inducing the diagnostic variable F_d to be 1, which indicates the accurate diagnosis of open-switch fault. In order to ensure the rapidity of the diagnosis as well as avoid a false detection under sudden load transient, a fault localization method is supplemented in the following section. It should be noted that the diagnostic variable F_d is not fixed after the fault, because the detection method is only to provide such a method. However in practical engineering, it can be maintained until the fault is located. In addition, regarding the experimental test with the change in the frequency, it is not required to detect the frequency of the currents, because the diagnostic variable in the detection method is independent of the frequency.

B. FAULT LOCALIZATION METHOD

The proposed method in the previous section can realize the fast detection when the fault of the inverter occurs, but it cannot determine the location of the fault power switch. Therefore, the fault location algorithm is proposed as described below.

The current zero-cross detection method is employed to avoid the influence of current distortion caused by load transient, where the sinusoidal current wave is converted to square wave. In order to avoid the error caused by the value near the threshold, a third level (zero) is introduced to improve the traditional zero-cross detection method. Here, we define:

$$\gamma_n(k) = \begin{cases} 1, & i_{nN}(k) \geq s_p \\ 0, & |i_{nN}(k)| < s_p \\ -1, & i_{nN}(k) \leq -s_p \end{cases} \tag{9}$$

where s_p is the threshold value. The selection of threshold value s_p must ensure the ability to locate the faulty switches in a wide range of loads. Nevertheless, it depends on several factors, such as switching frequency, dead time, current sensor offset, current signal to noise ratio, inverter topology

TABLE 1. The relationship between diagnosis variables and faulty switches.

Switches	F_d	Λ_a	Λ_b	Λ_c	$F_d*(\Lambda_a,\Lambda_b,\Lambda_c)$
Normal	0	0	0	0	(0,0,0)
T1	1	1	0	0	(1,0,0)
T2	1	-1	0	0	(-1,0,0)
T3	1	0	1	0	(0,1,0)
T4	1	0	-1	0	(0,-1,0)
T5	1	0	0	1	(0,0,1)
T6	1	0	0	-1	(0,0,-1)
T1&T4	1	1	-1	0	(1,-1,0)
T1&T6	1	1	0	-1	(1,0,-1)
T2&T3	1	-1	1	0	(-1,1,0)
T2&T5	1	-1	0	1	(-1,0,1)
T3&T6	1	0	1	-1	(0,1,-1)
T4&T5	1	0	-1	1	(0,-1,1)

configuration and so on. Therefore, s_p was chosen as approximately 2% of the rated current.

The fault localization can be based on the polarity of the motor phase currents. To achieve this goal, the polarity of the output currents can be described as the following relationship:

$$\Gamma_n(k) = \frac{\sum_{j=k-L}^{k} \gamma_n(j)}{\sum_{j=k-L}^{k} |\gamma_n(j)|} \tag{10}$$

where L represents the number of current samples per fundamental period, which is determined by the sampling frequency of dSPACE. The sampling values in each period are updated with the arrival of new sampling points. The value range of equation (9) is between -1 to 1. The value of equation (10) is approximately zero when the inverter works normally, but when a single switch fault or multiple switch open-switch fault occur, the value will be approximately 1 or -1. When the upper switch fails, its value is -1, and when the bottom switch fails, its value is 1. The fault flags are defined as:

$$\Lambda_n(k) = \begin{cases} 1, & \Gamma_n(k) \le -s_l \\ 0, & |\Gamma_n(k)| < s_l \\ -1, & \Gamma_n(k) \ge s_l \end{cases} \tag{11}$$

where s_l is the threshold value. When $\Lambda_n = 0$ it is under normal operating condition; when $\Lambda_n = 1$ there is an open-switch fault in the upper switch of phase n, and when $\Lambda_n = -1$ there is an open-switch fault in the bottom switch of phase n, which realizes open-switch fault localization of inverter. The threshold value s_l should be between 0 and 1. Taking into account a tradeoff between a fast diagnosis and the robustness against the issue false alarms, a small value can have a fast diagnosis speed, but a big value can be reliable.

Table 1 shows the relationship between the fault diagnosis variables and the fault power switch. The diagnostic method in this paper can diagnose 12 distinct signatures using Table 1.

IV. EXPERIMENTAL RESULTS

In this section, the experimental setup is set up to verify the fault diagnosis algorithm of the open-switch switch fault mentioned, as shown in Fig. 3. The experimental setup includes the three-phase two-level voltage source inverter feeding LC filter and resistive loads, dSPACE controller. The dSPACE controller, together with Matlab/Simulink and dSPACE ControlDesk software, allows providing functions for real-time control and monitoring of the inverter and capturing the data files. The system parameters used for the experimental test are shown in Table 2.

TABLE 2. System parameters.

DC-link voltage	V_{dc}	*30V*
Filter inductances	L_a, L_b, L_c	*13mH*
Filter capacitors	C_a, C_b, C_c	*10μF*
Loads	R_a, R_b, R_c	*20Ω*
Current fundamental period	T	*20ms*
Switching frequency	f_s	*10kHz*
Sampling period	t_{sample}	*100μs*

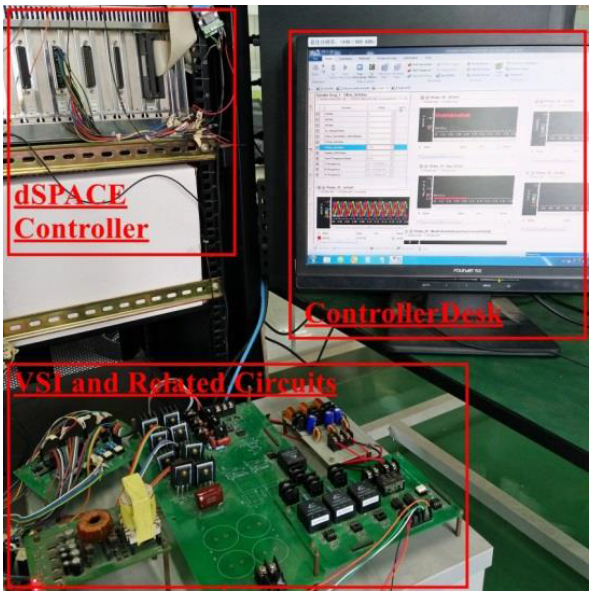

FIGURE 3. Experimental setup.

The experimental results are showed to evaluate the diagnostic method performance under different failure conditions. In this section, single open-switch fault and double open-switch fault are considered, and the immunity to false alarms is verified as a consequence of load and current frequency transients. The threshold values s_d, s_p, s_l are set to be equal to 1.8, 0.02, and 0.3 in the experiments, respectively.

A. FAULT DETECTION AND LOCALIZATION

Fig. 4 shows the experimental results when open-switch fault happens to T4 at t = 67.8145s. Under normal operating conditions, it can be seen that the currents are sinusoidal, which gets a null value for the diagnostic variables F_d and Λ_a, Λ_b, Λ_c since the actual currents follow their corresponding reference signals. However, after open-switch fault happens to T4 at the instant t = 67.8155s the phase current b becomes null during the negative half-cycle immediately, and as a result, the detection variable $\langle\rho\rangle$ decreases below s_d at

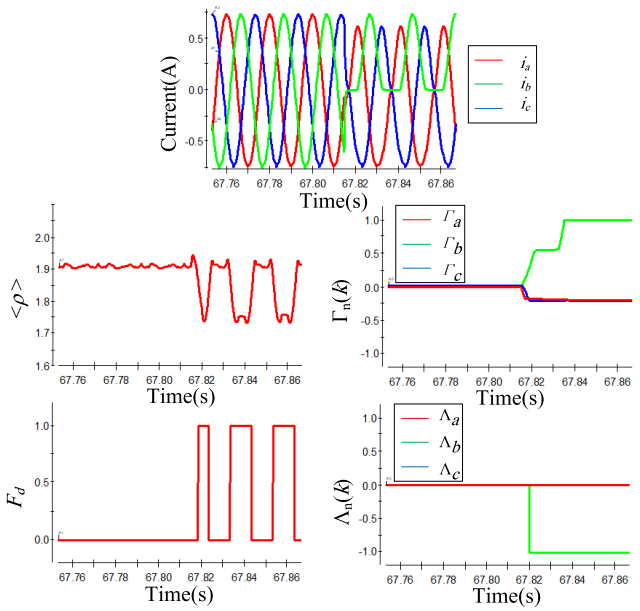

FIGURE 4. Experimental results for an open-switch fault In T4.

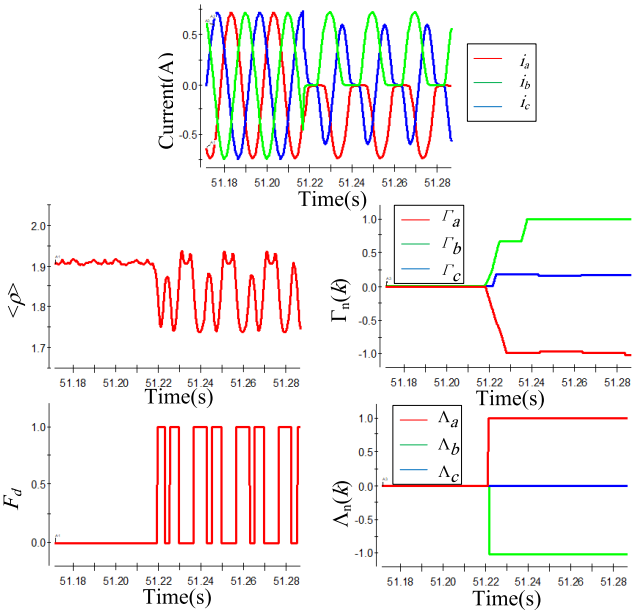

FIGURE 5. Experimental results for double switch faults in T1 and T4.

t = 67.818s and the localization variable Γ_b increases above s_l at t = 67.8195s, allowing for the identification of the faulty switch T4. And the detection and localization times correspond to approximately 12.5% and 20% of the currents fundamental period, respectively.

Fig. 5 shows the experimental results for double switch faults, where the open-switch faults occur in T1 and T4. At the instant t = 51.217s, the faults occur. It can be see that the values of the faulty phase a will have negative value, while the phase b value becomes positive the faults occur. The detection variable $\langle\rho\rangle$ immediately decreases below s_d after the failure occurs, and the detection time is 2ms which is approximately 10% of the currents fundamental period. Besides the localization variable Γ_a decreases below $-s_l$ and Γ_b increases above s_l after the failure occurs less than 4ms, which is approximately 20% of the currents fundamental period, allowing for the identification of the faulty switches T1 and T4.

B. TRANSIENTS BEHAVIOR

The detection and localization variables are responsible to ensure the robustness to transients and prevent their misinterpretation under the transient condition, although all of the switches are operated in a normal state.

Fig. 6(a) and (b) presents the time-domain waveforms of the phase currents, the fault detection and localization variables during several load transients.

In Fig. 6(a), the loads Ra, Rb and Rc decrease from 25Ω to 10Ω at t = 215.82s, which results in the increase of currents. The amplitude of current increases from 0.6A to 1.3A, which about varies by 216.7%. At the meantime, the detection variable $\langle\rho\rangle$ varies slightly in the range of normal operating condition. It can be firmly convinced that there is no false alarm when the load decreases. At t = 216.28s the loads

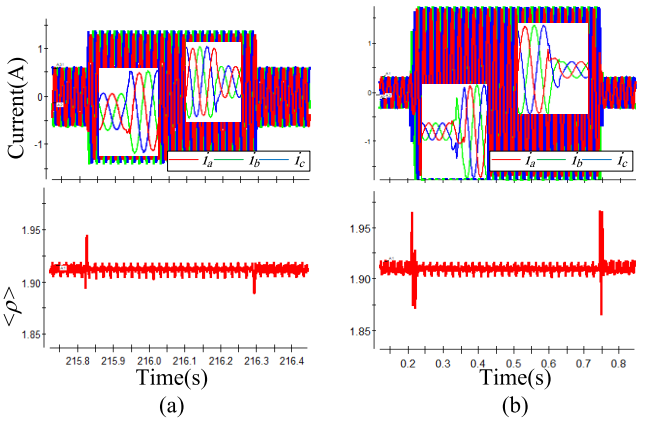

FIGURE 6. Experimental results during load transients.

increase from 10Ω to 25Ω, which results in the decrease of currents. The amplitude of current changes from 0.6A to 1.3A, which about varies by 46.15%. At the same time, the value of $\langle\rho\rangle$ varies slightly above the threshold value s_d, and the detection variable F_d still remains zero, and it does not cause false alarm when the loads increase. During the load transient, the value of $\langle\rho\rangle$ varies slightly above the threshold values_d, the detection variables F_d still remain zero, and it does not cause false alarm.

In Fig. 6(b), the load Ra, Rb, Rc decrease from 50Ω to 7Ω at t = 0.2s and back to 50Ω at t = 0.75s, which results the amplitude of current changes from 0.35A to 1.75A and back to 0.35A, which about varies by 20% and 500%, respectively. Although the load transients greatly, the value of $\langle\rho\rangle$ varies slightly in the range of normal operating condition and the detection variable F_d still remains zero. It can be firmly convinced that there is no false alarm when the loads decrease or increase.

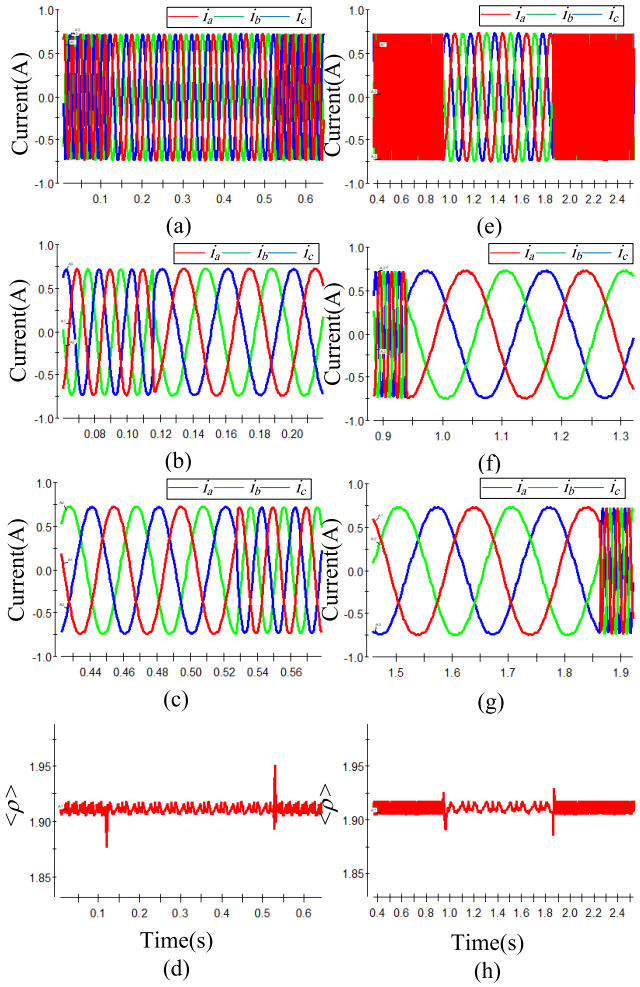

FIGURE 7. Experimental results during current frequency variation.

After repeated experiment verification, when the load changes in the range of 20%-500%, the value of $\langle\rho\rangle$ varies slightly above the threshold value, there is no false alarm. By comparing the results of experiment and simulation, it is found that the results are the same and the experiment results and the simulation results are in good agreement with the theoretical analysis. It can be seen that the proposed detection method has good resistance to load variation.

Fig. 7 presents the time-domain waveforms of the phase currents, the fault detection and localization variables during the current frequency variation.

In Fig. 7(a)-(d), the current frequency decrease from 50Hz to 25Hz at t = 0.115s and back to 50Hz at t = 0.53s, which about varies by 50% and 200%, respectively. In Fig. 7(b), the current frequency decrease from 50Hz to 5Hz at t = 0.115s, which about varies by 10%. Fig. 7(c), the current frequency decrease from 5Hz to 50Hz at t = 0.53s, which about varies by 1000%. In Fig. 7(e)-(h), the current frequency decrease from 50Hz to 5Hz at t = 0.94s and back to 50Hz at t = 1.86s, which about varies by 50% and 200%, respectively. In Fig. 7(f), the current frequency decrease from 50Hz to 5Hz at t = 0.115s, which about varies by 10%. Fig. 7(g), the current frequency decrease from 5Hz to 50Hz at t = 0.53s, which

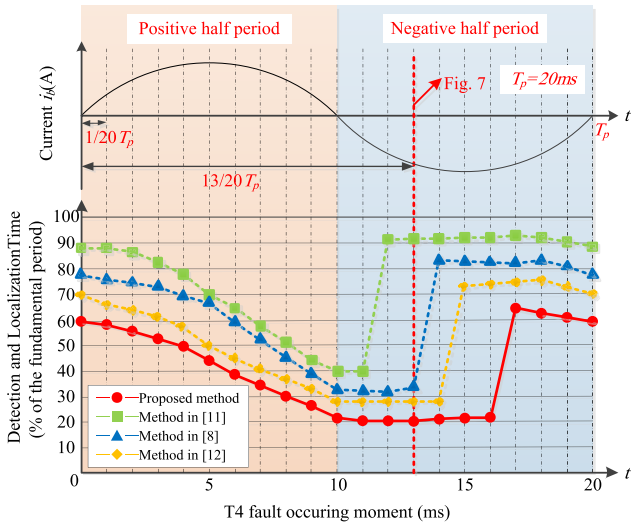

FIGURE 8. Detection and localization time when T4 fault occurs at 20 evenly-spaced moments in a fundamental period.

about varies by 1000%. Although the current frequency varies greatly, the value of $\langle\rho\rangle$ varies slightly in the range of normal operating condition in Fig. 7(d) and (h), and the detection variable F_d still remains zero. It can be firmly convinced that there is no false alarm when the current frequency decreases or increases. After repeated experiments verification, when the current frequency changes in the range of 10%-1000%, the value of $\langle\rho\rangle$ varies slightly above the threshold value, there is no false alarm.

In order to give an overview of diagnosis speed, the diagnosis time of the proposed method for single faults is investigated comparing to several methods in [8], [11] and [12]. By repeating experiments, the detection and localization time for faults occurring to T4 at 20 evenly-spaced moments in a fundamental period is shown in Fig.10. T_p represents the fundamental period. For instance, when the fault occurs at 13/20 T_p in Fig.8, the detection and localization time of proposed method is about 20% of the currents fundamental period. Similar conclusion can be drawn by repeating experiments in [8], [11] and [12]. To sum up, the proposed method shows better performance in the detection and localization speed. For the same fault, detection and location takes less time and has a faster speed.

V. CONCLUSION

The diagnosis method has been introduced for the detection and localization of open-switch faults of three-phase voltage-source inverter. The current zero-cross detection method and the fault detection signal based on the phase currents are built to precisely localize the faulty switches. The single and double switches open faults can be detected and localized by 12 distinct fault signatures corresponding to a unique inverter failure combination. Regarding the diagnostic method detection speed, the simulation and experiment results show that a faulty switch can be detected within a time equivalent to one eighth of the current fundamental period, which can be considered, comparing with similar techniques, relatively fast.

In addition, the diagnosis method has the ability to ensure the robustness to the transient condition, such as load variations and current frequency variations, and prevent misinterpretation under the transient condition.

REFERENCES

[1] S. Yang, D. Xiang, A. Bryant, P. Mawby, L. Ran, and P. Tavner, "Condition monitoring for device reliability in power electronic converters: A review," *IEEE Trans. Power Electron.*, vol. 25, no. 11, pp. 2734–2752, Nov. 2010.

[2] W. Zhang, D. Xu, P. N. Enjeti, H. Li, J. T. Hawke, and H. S. Krishnamoorthy, "Survey on fault-tolerant techniques for power electronic converters," *IEEE Trans. Power Electron.*, vol. 29, no. 12, pp. 6319–6331, Dec. 2014.

[3] M. Gu *et al.*, "A SiC-based T-type three-phase three-level gridtied inverter," in *Proc. IEEE 10th Conf. Ind. Electron. Appl.*, Jun. 2015, pp. 1116–1121.

[4] U.-M. Choi, H.-G. Jeong, K.-B. Lee, and F. Blaabjerg, "Method for detecting an open-switch fault in a grid-connected NPC inverter system," *IEEE Trans. Power Electron.*, vol. 27, no. 6, pp. 2726–2739, Jun. 2012.

[5] H. Zhao and L. Cheng, "Open-switch fault-diagnostic method for back-to-back converters of a doubly fed wind power generation system," *IEEE Trans. Power Electron.*, vol. 33, no. 4, pp. 3452–3461, Apr. 2018.

[6] T. Shi, Y. He, F. Deng, J. Tong, T. Wang, and L. Shi, "Online diagnostic method of open-switch faults in PWM voltage source rectifier based on instantaneous AC current distortion," *IET Electr. Power Appl.*, vol. 12, no. 3, pp. 447–454, Mar. 2018.

[7] Q. Yang, J. Qin, and M. Saeedifard, "Analysis, detection, and location of open-switch submodule failures in a modular multilevel converter," *IEEE Trans. Power Del.*, vol. 31, no. 1, pp. 155–164, Feb. 2016.

[8] W. Sleszynski, J. Nieznanski, and A. Cichowski, "Open-transistor fault diagnostics in voltage-source inverters by analyzing the load currents," *IEEE Trans. Ind. Electron.*, vol. 56, no. 11, pp. 4681–4688, Nov. 2009.

[9] C. Cecati, A. O. D. Tommaso, F. Genduso, R. Miceli, and G. R. Galluzzo, "Comprehensive modeling and experimental testing of fault detection and management of a nonredundant fault-tolerant VSI," *IEEE Trans. Ind. Electron.*, vol. 62, no. 6, pp. 3945–3954, Jun. 2015.

[10] D. U. Campos-Delgado and D. R. Espinoza-Trejo, "An observer-based diagnosis scheme for single and simultaneous open-switch faults in induction motor drives," *IEEE Trans. Ind. Electron.*, vol. 58, no. 2, pp. 671–679, Feb. 2011.

[11] N. J. O. F. Estima and A. J. M. Cardoso, "Open-switch fault diagnosis in PMSG drives for wind turbine applications," *IEEE Trans. Ind. Electron.*, vol. 60, no. 9, pp. 3957–3967, Sep. 2013.

[12] J. O. Estima and A. J. M. Cardoso, "A new approach for real-time multiple open-circuit fault diagnosis in voltage-source inverters," *IEEE Trans. Ind. Appl.*, vol. 47, no. 6, pp. 2487–2494, Nov./Dec. 2011.

[13] J. O. Estima and A. J. M. Cardoso, "A new algorithm for real-time multiple open-circuit fault diagnosis in voltage-fed PWM motor drives by the reference current errors," *IEEE Trans. Ind. Electron.*, vol. 60, no. 8, pp. 3496–3505, Aug. 2013.

[14] D. R. Espinoza-Trejo, D. U. Campos-Delgado, and G. Bossio, "Fault diagnosis scheme for open-circuit faults in field-oriented control induction motor drives," *IET Power Electron.*, vol. 6, no. 5, pp. 869–877, 2013.

[15] I. Jlassi, J. O. Estima, S. K. El Khil, N. M. Bellaaj, and A. J. M. Cardoso, "Multiple open-circuit faults diagnosis in back-to-back converters of PMSG drives for wind turbine systems," *IEEE Trans. Power Electron.*, vol. 30, no. 5, pp. 2689–2702, May 2015.

[16] I. Jlassi, J. O. Estima, S. K. El Khil, N. M. Bellaaj, and A. J. M. Cardoso, "A robust observer-based method for IGBTs and current sensors fault diagnosis in voltage-source inverters of PMSM drives," *IEEE Trans. Ind. Appl.*, vol. 53, no. 3, pp. 2894–2905, May/Jun. 2017.

[17] H. Jian-Ding, Q. Rong, Z. Jian-Ye, L. Xiao-Ben, and W. Chen, "Fault diagnosis for power electronic circuits based on mixed logic dynamic model and identification vector," in *Proc. IEEE Asia–Pacific Power Energy Eng. Conf. (PES)*, Oct. 2016, pp. 502–508.

[18] O. Moseler and R. Isermann, "Application of model-based fault detection to a brushless DC motor," *IEEE Trans. Ind. Electron.*, vol. 47, no. 5, pp. 1015–1020, Oct. 2000.

[19] C.-J. Bae, S.-M. Lee, and D.-C. Lee, "Diagnosis of multiple IGBT open-circuit faults for three-phase PWM inverters," in *Proc. IEEE 8th Int. Power Electron. Motion Control Conf.*, May 2016, pp. 2504–2509.

[20] R. Szczesny, P. Kurzynski, H. Piqueb, and K. Hwan, "Knowledge-base system approach to power electronic systems fault diagnosis," in *Proc. IEEE Int. Symp. Ind. Electron.*, vol. 2, Jun. 1996, pp. 1005–1010.

[21] M. R. Mamat, M. Rizon, and M. S. Khanniche, "Fault detection of 3-phase VSI using wavelet-fuzzy algorithm," *Amer. J. Appl. Sci.*, vol. 3, no. 1, pp. 1642–1648, 2006.

[22] M. Aktas and V. Turkmenoglu, "Wavelet-based switching faults detection in direct torque control induction motor drives," *IET Sci. Meas. Technol.*, vol. 4, no. 6, pp. 303–310, Nov. 2010.

[23] K. Rothenhagen and F. W. Fuchs, "Performance of diagnosis methods for IGBT open circuit faults in voltage source active rectifiers," in *Proc. IEEE 35th Annu. Power Electron. Spec. Conf. (PESC)*, vol. 6, Jun. 2004, pp. 4348–4354.

[24] M. Shahbazi, E. Jamshidpour, P. Poure, S. Saadate, and M. R. Zolghadri, "Open- and short-circuit switch fault diagnosis for nonisolated DC–DC converters using field programmable gate array," *IEEE Trans. Ind. Electron.*, vol. 60, no. 9, pp. 4136–4146, Sep. 2013.

[25] C. Brunson, L. Empringham, L. De Lillo, P. Wheeler, and J. Clare, "Open-circuit fault detection and diagnosis in matrix converters," *IEEE Trans. Power Electron.*, vol. 30, no. 5, pp. 2840–2847, May 2015.

ZHANG JIAN-JIAN was born in Henan, China, in 1993. He received the B.S. degree in electrical engineering and its automation from the University of Electronic Science and Technology of China (UESTC), in 2016, where he is currently pursuing the M.S. degree in electrical engineering. His research interests include fault diagnosis and fault-tolerant control in voltage-source inverter.

CHEN YONG (M'08–SM'16) was born in Sichuan, China, in 1977. He was Visiting Scholar with The University of Adelaide, in 2013. Since 2015, he has been a Professor and a Ph.D. Supervisor with the School of Automation Engineering and the Director of the Institute for Electric Vehicle Driving System and Safety Technology, University of Electronic Science and Technology of China (UESTC). He has published over 100 technical papers in journals and conferences, and holds 20 Chinese patents. His research interests include power electronics, motor control, fault-torrent control, and network control.

CHEN ZHANG-YONG was born in Sichuan, China, in 1988. He received the B.S. degree in electrical engineering and its automation and the Ph.D. degree in electrical engineering from Southwest Jiaotong University (SWJTU), Chengdu, China, in 2010 and 2015, respectively. He was a Visiting Student with Virginia Tech, Blacksburg, in 2014. He is currently an Associate Professor with the School of Automation Engineering, University of Electronic Science and Technology of China (UESTC). His research interests include switching-mode power supplies, soft switching techniques, power factor correction converters, and renewable energy sources.

ZHOU ANJIAN was born in Sichuan, China, in 1967. He received the B.S. degree from the Taiyuan Institute of Machinery University, China, in 1991, and the M.S. degree from Chongqing University, China, in 2010. He is currently a Professor, a Senior Engineer, and the Vice Manager of Chongqing Changan New Energy Automobile Technology Co., Ltd., and the General Manager of the Propulsion Development Department. His current research interests include new energy vehicles and electric vehicles.